JOURNAL OF MATERIALS SCIENCE 32 (1997) 1855–1860

Mechanisms of cavitation over a range of temperatures in rubber-toughened PSAN modified with three-stage core–shell particles

J.U. STARKE, R. GODEHARDT, G.H. MICHLER
Department of Materials Science, Martin-Luther-University Halle-Wittenberg, Geusaer Straße, D-06217 Merseburg, Germany

C. B. BUCKNALL
Advanced Materials Group, Cranfield University, Cranfield, Bedford, MK43 0AL, UK

In situ straining on a transmission electron microscope (TEM) stage has been used to study deformation mechanisms in a blend of poly(styrene-co-acrylonitrile) (PSAN) with PMMA/acrylate-rubber/PMMA core–shell particles, over a range of temperatures. Thin sections were tested at -20, 23 and 60 °C at a constant tensile strain rate of 0.05% s^{-1}. Cavitation was observed at all three temperatures. At -20 °C, the main deformation mechanisms were crazing of the PSAN matrix and fibrillation of the acrylate rubber. At 23 °C, crazing and shear yielding of the PSAN occurred simultaneously, with more extensive fibrillation of the rubber particles and drawing of material from the PMMA cores. This disruption of thermoplastic core material indicates that high stresses are generated within the modifier particles. At 60 °C, crazing could no longer be detected: shear yielding of the matrix and cavitation of the rubber particles were the main mechanisms of deformation.

1. Introduction

A well established procedure for improving the impact strength of glassy polymers is to incorporate a dispersed rubbery phase [1–3]. Very fine and well dispersed morphologies can be obtained by blending the glassy polymer with core–shell particles. In the simplest case, these consist of a lightly-crosslinked elastomeric core to which is grafted a rigid glassy shell, typically of poly(methyl methacrylate) (PMMA). Alternatively, in a three-stage core–shell particle, the core is a glassy polymer, the inner grafted shell is elastomeric, and the outer grafted shell is a glassy polymer. These special modifier particles are produced by emulsion polymerization [4–6] and compounded in a second step with the matrix polymer.

Under tension, soft modifer particles act as stress concentrators, initiating energy absorbing deformation processes in the matrix polymer. Depending on external conditions (temperature, mode and rate of deformation) and morphological parameters (particle diameter, interparticle distance, rubber volume content) PSAN blends deform by different combinations of crazing and shear yielding [1, 2].

Over the past few years another deformation mechanism has received increasing attention. Bubeck *et al.* [7] have demonstrated that significant amounts of non-craze voiding occur during tensile impact testing of ABS and high-impact polystyrene (HIPS), beginning just before the yield point and continuing up to failure. *In situ* TEM studies [8] have shown that this non-craze voiding can be attributed to cavitation of the rubber particles, particularly in certain PSAN blends, where cavitation of the rubber particles is the main micro-mechanical deformation process. Cavitation is concentrated into planar regions, producing craze-like structures which have been called "croids" (from *craze-void*). These are dilatation bands formed on planes perpendicular to the tensile stress direction, within which yielding of the matrix polymer is accelerated by the presence of cavitated rubber particles. Similar craze-like structures formed through cavitation of the rubber phase have been observed by Argon *et al.* [9] in styrene–butadiene block copolymers. There are significant differences between crazes and dilatation bands. Crazes are open-celled structures in which the void regions are continuous, whereas "croids" and other types of dilatation band in rubber-toughened plastics are closed-celled structures in which the cavitated rubber particles are separated from each other by a continuous zone of plastically deformed matrix polymer. This difference can have a strong effect upon mechanical properties in the presence of active environments [10]. In blends of semi-crystalline matrix with rubber, cavitation of the rubber particles can initiate numerous energy-absorbing shear bands [11, 12] which connect the voids and increase toughness. The effects of particle cavitation in toughened plastics have been analysed in detail by Lazzeri and Bucknall [13].

Numerous optical and electron microscopic studies have been published on the micro-mechanical deformation of rubber-toughened plastics at room

0022–2461

temperature. *In situ* dynamic tensile tests on the stage of a high-voltage electron microscope (HVEM) are particularly effective because the method combines the advantage of relatively thick samples (thicker than the modifier particle diameter) with a high resolution [14–17]. However, for many industrial applications of polymer blends, information is also necessary on toughening mechanisms at low temperatures. The aim of the present study is to analyse details of plastic deformation in a PSAN–rubber blend over a range of temperatures and strain rates, from the onset of yielding to crack propagation, using *in situ* TEM.

2. Material

The PSAN matrix material used to prepare the blend was Montefluos Kostil AP 600, which was melt compounded with 20 vol % of ICI Diakon XC 42 core–shell rubber particles. These particles consist of a single core of poly(methyl methacrylate) (PMMA), surrounded by a 20 nm thick inner shell of grafted and lightly cross-linked poly(butyl acrylate-co-styrene) and an outer grafted shell of glassy PMMA. This PMMA layer is about 10 nm thick, and is sufficiently miscible with PSAN to provide good adhesion between the matrix and the modifier particle. For simplicity, the whole modifier will be designated PBA modifier. The glass transition temperature T_g for the poly(butyl acrylate-co-styrene) elastomer phase, measured by dynamic mechanical analysis, lies at approximately $-10\,^{\circ}C$. The PBA modifier particles have an average particle diameter of about 300 nm and a narrow distribution of diameters, as illustrated in Fig. 1.

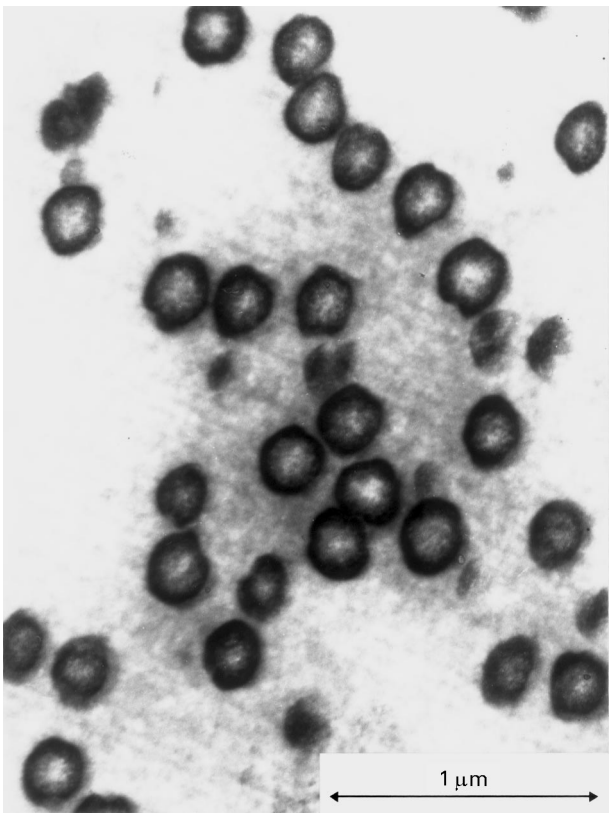

Figure 1 Morphology of core–shell particles in the SAN/PBA blend stained with Rutheniumtetroxid (RuO_4); (TEM micrograph).

The PBA phase in this micrograph appears dark owing to staining with RuO_4. A small percentage of particles was as large as 500 nm, with a more complex core–shell morphology (more than one PBA and PMMA layer). The PSAN and PBA were melt-blended in a co-rotating twin-screw compounding extruder at $260\,^{\circ}C$.

3. Experimental details

In situ tensile experiments were carried out in the high-voltage electron microscope (HVEM) in order to characterize deformation processes at room temperature. Approximately the same strain rate was used in all tests, but its actual value is unknown. Specimen preparation and experimental operation with the 1000 kV high-voltage electron microscope (HVEM) have been described in detail elsewhere [18, 19]. The higher acceleration voltage in the HVEM leads to a lower inelastic scattering of the electrons by the matrix material. Consequently, the thickness of the specimens can be increased and irradiation damage decreased. Micro-mechanical deformation tests in the HVEM are restricted to room temperature because of the special construction of the tensile device.

In the last few years, a new method has been used to investigate dynamic plane stress failure of polymer blends, especially at low temperatures, using a single-tilt cooling/straining holder (Gatan Inc.) [20, 21]. Such a holder makes it possible to deform thin sections at temperatures between -170 and $+120\,^{\circ}C$ at constant strain rates. Specimens were sectioned from the bulk at $-110\,^{\circ}C$ using a cryo-ultramicrotome "Ultracut E" (Leica GmbH). These relatively stable sections are glued between two adhesive metallic films to provide a "sample/metallic-film sandwich". Afterwards the "sandwich" is mounted in the tensile holder. Using a 200 kV transmission electron microscope (Jeol Inc.), sections or films about 0.3 μm thick can be investigated. The resolution of TEM micrographs, which is important in studying details of deformation structure, is higher than that of HVEM micrographs. Irradiation damage to thinner specimens can be reduced by altering the manner of operation (e.g. using low dose techniques [20]).

Cieslinski [21] also used a cooling/straining TEM stage to study brittle/ductile transitions in rubber toughened plastics over a range of test temperatures. In his experiments, the material was impact polypropylene (PP). In contrast to our preparation method, Cieslinski needed several, specially designed cartridges to deform thin sections of impact PP in tension on the stage of the TEM. Consequently, his test temperatures were restricted to the range -170 to $23\,^{\circ}C$.

4. Results and discussion

Fig. 2 is a HVEM micrograph showing the characteristic deformation behaviour of stretched PSAN/PBA blends in semi-thick sections (about 1.5 μm thick). In unstained sections of this type, the contrast between particles and matrix is obtained from the "strain

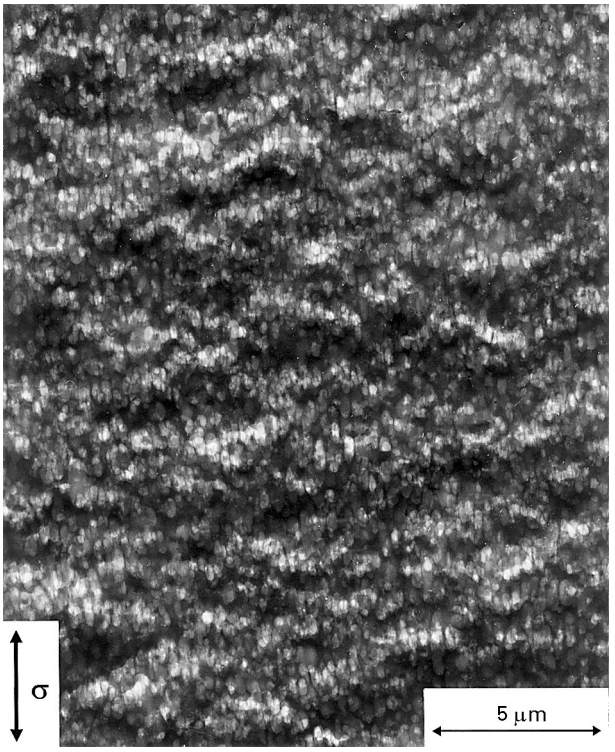

Figure 2 Deformation structure in the SAN/PBA blend at relatively low magnification showing the coexistence of homogenous shear deformation between particles and crazes at room temperature; (HVEM micrograph, deformation direction see arrow).

induced contrast enhancement" effect described in [18]. Rubber particles and plastic deformation zones in the matrix are thinner and therefore appear brighter than the elastically-deformed matrix material. At the low magnification shown in Fig. 2, the micro-mechanical deformation process in the PSAN/PBA blend at room temperature seems to be mainly homogeneous shear deformation of the matrix material between the particles. At higher magnifications, it can be seen that a small number of short and relatively thin crazes is also formed. This mixture of shear deformation and crazing is characteristic of PSAN blends at room temperature [1, 2].

It is well known that strain rate and temperature have a strong effect on the deformation behaviour of rubber-toughened plastics. Owing to the limited capability of the HVEM to investigate these variables, a 200 kV TEM fitted with the cooling/straining specimen holder described above was used for the main part of this study.

4.1. Effect of test temperature

Fig. 3 compares micrographs of thin sections subjected to *in situ* tensile tests at -20, 23 and 60 °C at a constant strain rate of 0.05 s^{-1}. They show an obvious change in deformation behaviour with temperature. At -20 °C (Fig. 3a), the main mechanisms are crazing of the PSAN and fibrillation of the elastomeric shells of the PBA particles, around their PMMA cores. The bright crazes show up clearly against the dark background of the undeformed matrix and the paler grey of the moderately-stretched modifier particles. The PBA particles are relatively hard, because the T_g of the poly(butyl acrylate) copolymer shells lies between -10 and -15 °C. Only the larger particles and small groups of closely-spaced particles are able to cavitate and initiate crazes. The specimens broke in a brittle manner on the TEM stage.

At 23 °C, above the T_g of the rubbery phase, nearly all of the particles cavitate (Fig. 3b). The shear yield stress of PSAN is lower than at -20 °C, so that shear deformation mechanisms become more apparent, and the contribution of crazes to tensile extension decreases. The strain at break (ε_B) of the 300 nm thick sections increases to about 40%. The appearance of these thin tensile specimens in the 200 kV TEM is comparable to that of semi-thick sections subjected to tensile tests in the HVEM at room temperature, showing a combination of crazing and shear deformation (cf. Fig. 2).

At 60 °C (Fig. 3c), there is very little evidence of crazing; the matrix deforms almost exclusively by shear deformation. The PBA particles cavitate, leaving thin membranes of polymer spanning the gaps. The PMMA cores visible in Fig. 3a are nowhere to be seen in Fig. 3c, and appear to be completely disrupted at the higher test temperature. The PSAN/PBA blend specimens deform in a ductile manner on the TEM stage.

4.2. Cavitation mechanisms

The cavitation mechanism within the modifier particles is quite different at 60 °C from that at 23 °C. The differences are caused by the distinctive morphology of the modifier and by thermal softening the individual polymeric phases. At 23 °C and strain rates of 0.05 s^{-1} the cavitation process begins with fibrillation of the butyl acrylate copolymer layer, as shown in Fig. 4. One or two of the glassy PMMA cores appear to be elongated in the tensile stress direction, but they remain intact. The cavitated modifier particles resemble spiders. In most cases, the PMMA cores are not located in the middle of the fibrillated material. The average lengths of the PBA fibrils are about 200 nm, which in relation to the thickness of the undeformed PBA layer (about 20 nm) corresponds to an extension ratio of $\lambda \cong 10$. Normally, the extension ratios of relatively weak cross-linked polymers reach values of 4 to 5. Extension ratios of $\lambda \cong 10$ suggest that the fibrils are not formed exclusively from the butyl acrylate copolymer inner shell, but also incorporate some polymeric material from the PMMA core and/or from the PMMA outer shell, possibly extending into the PSAN matrix.

This hypothesis is supported by HVEM observations on 0.75 μm thick sections at relatively high strains. Fig. 5 shows a pattern of light-coloured deformation bands formed as a result of crazing in the PSAN and cavitation of the rubber particles. Most of these particles feature a dark lens-shaped inclusion, apparently formed from the PMMA core. Contrary to expectation, the axes of these lenses are oriented perpendicular to the tensile stress direction. This phenomenon can be explained only on the assumption

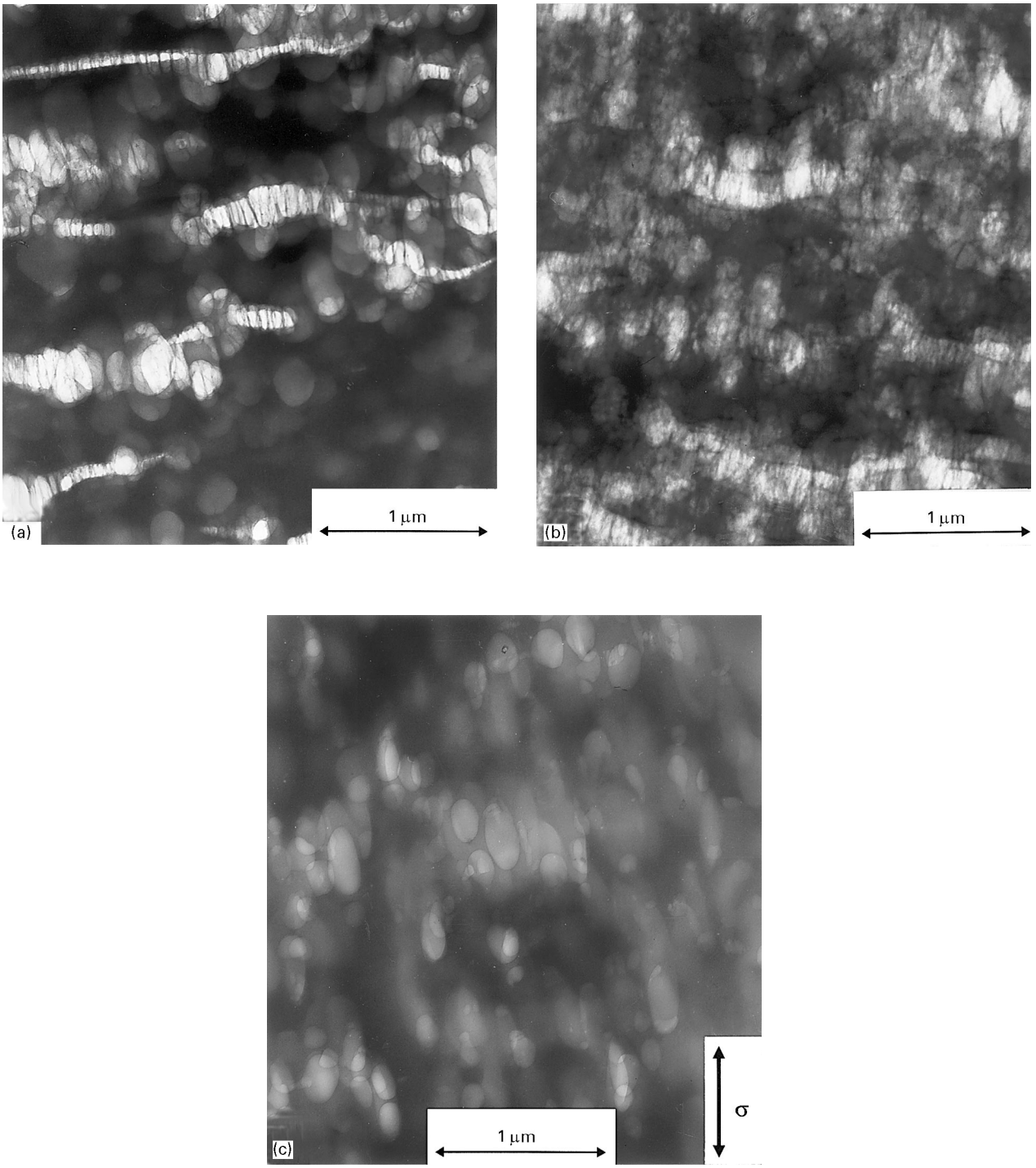

Figure 3 Deformation structures in the SAN/PBA blend at various temperatures and constant strain rate of $0.05\,s^{-1}$; (a) $-20\,^{\circ}C$, (b) $+23\,^{\circ}C$, (c) $+60^{\circ}C$ (TEM micrographs, deformation direction see arrow).

that theremoplastic PMMA is drawn from the core of each particle as the test progresses to high tensile strains. Fibrils lying close to the direction of maximum strain need the greatest amount of core material to accommodate the large extensions in the matrix. Therefore, the caps of the cores, defined with respect to the tensile direction, are strongly disrupted. These regions of the PMMA core appear to lose their glassy properties, in similar manner to that seen in craze formation [22–25].

It is clear from this evidence that the stresses operating within the fibrillated modifier particles are relatively high, since nominal stresses in the order of 30–50 MPa are necessary to draw fibrils from the wall of a PMMA craze at 23 °C, and the stresses required to cause drawing by a shear mechanism are higher still. It is possible that heating in the electron beam raised the temperature of the section above 23 °C, but at any temperature substantially below the T_g of PSAN, which is close to its own T_g, PMMA is relatively resistant to plastic deformation.

By contrast, no such spider-like structures are observed in modifier particles cavitated at 60 °C, as illustrated in Fig. 6. The experimental conditions, and in particular the increased temperature, cause an increase in molecular mobility not only in the PSAN

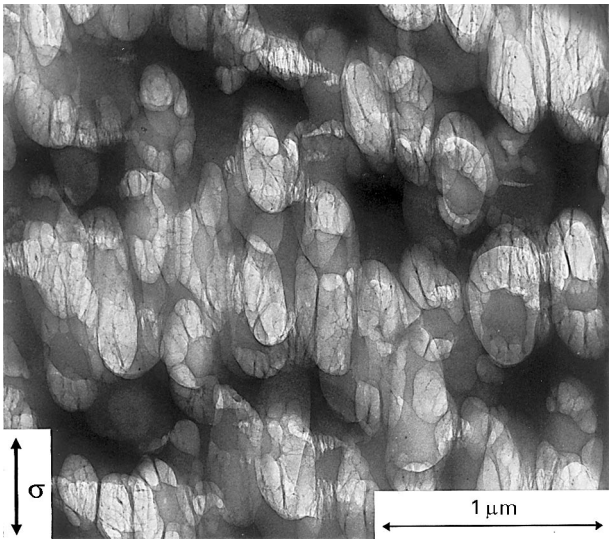

Figure 4 Cavitation mechanisms of core–shell modifier particles in the SAN/PBA blend at + 23 °C; (TEM micrographs, deformation direction see arrow).

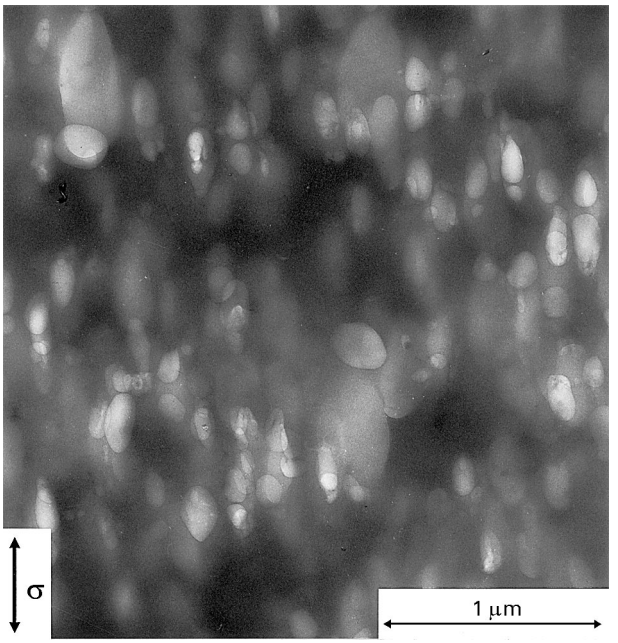

Figure 6 Cavitation mechanisms of core–shell modifier particles in the SAN/PBA blend at + 60 °C; (TEM micrograph, deformation direction see arrow).

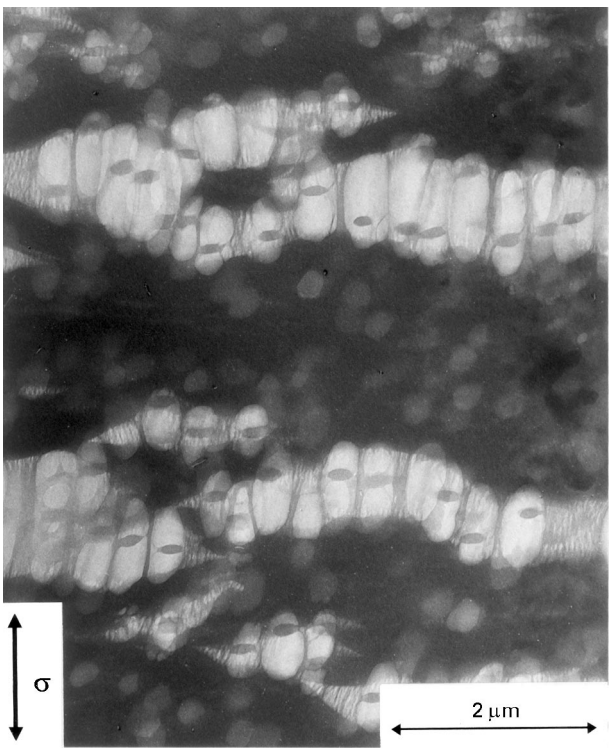

Figure 5 Deformation structure at relatively high strain levels and room temperature showing flattened PMMA cores within cavitated modifier particles; (HVEM micrograph, deformation direction see arrow).

matrix but also in the PMMA cores of modifier particles, with the result that the thermoplastic cores are completely disrupted at high strains, and each modifier particle appears to form a single large cavity, bridged by one or two weak membranes of polymer. Large elongations of voids at relatively high temperatures accompany large deformations in the PSAN matrix by drawing or shear yielding, indicating that the blend is very tough in tensile tests at 60 °C.

4.3. Effect of strain rate

The deformation behaviour of the PSAN/PBA blend was investigated at 23°C and at three strain rates: 0.01, 0.05 and 0.1 s^{-1}. These tests showed that strain rate only had a small influence. In each case, extension occurred through a combination of crazing and shear yielding, similar to that shown in Fig. 3b.

5. Conclusions

Deformation mechanisms in a blend of PSAN with a three-stage core–shell PBA modifier have been investigated by means of tensile tests carried out *in situ* in the 1000 kV HVEM and in a 200 kV TEM at various temperatures and strain rates. The modifier has a rigid PMMA core, a rubbery poly(butadiene-co-styrene) inner shell, and a rigid PMMA outer shell.

The micro-mechanical deformation processes observed at 23°C in 1.5 μm thick sections deformed *in situ* in the HVEM are similar to those seen in 300 nm thick sections in the 200 kV TEM, with the PSAN matrix extending by a combination of crazing and shear deformation, and the rubber particles undergoing cavitation to form fibrils which are connected and stabilized by the PMMA core. One, possibly significant, difference between the two sets of observations is that a section strained in the HVEM shows evidence of disruption of the PMMA cores of the modifier particles, leaving residual lens-shaped cores, whereas this behaviour has as yet not been observed in thinner sections strained in the 200 kV TEM.

There is a transition in the deformation behaviour on lowering the temperature from 23 to − 20 °C, where craze formation is the main deformation process. A second transition occurs between 23 and 60 °C: at the higher temperature, the PSAN matrix deforms almost exclusively by shear yielding, and the modifier

particles are completely disrupted on cavitation, leaving little visible evidence of the presence of rigid cores.

Acknowledgements

The authors thank Professor J. Heydenreich for the opportunity to carry out deformation tests in the 1000 kV high-voltage electron microscope in the Max-Planck-Institut für Mikrostrukturphysik, Halle. They are also grateful to the Max-Buchner-Forschungsstiftung for financial support for J. U. Starke; the British Council and the Deutscher Akademischer Austauschdienst for travel funds; and G. Harlammert (Hüls AG) for studies of morphology. This study forms part of a research programme conducted by IUPAC Working Party 4.2.1. Further details of the programme will be published in Pure & Applied Chemistry.

References

1. G. H. MICHLER, "Kunststoff-Mikromechanik: Morphologie, Deformations- und Bruchmechanismen" (Carl Hanser Verlag, München, Wien, 1992).
2. C. B. BUCKNALL, "Toughened Plastics" (Applied Science, London, 1977).
3. A. J. KINLOCH and R. J. YOUNG, "Fracture Behaviour of Polymers" (Elsevier Applied Science Publishers, London, New York, 1983).
4. P. A. LOVELL, J. MC DONALD, D. E. J. SAUNDERS and R. J. YOUNG, *Polymer* **34** (1993) 61.
5. M. OKUBO, *Makromol. Chem. Macromol. Symp.* **35**/**36** (1990) 307.
6. D. R. STUTMAN, A. KLEIN, M. S. EL-AASSER and J. W. VANDERHOFF, *Ind. Eng. Chem. Prod. Res. Dev.* **24** (1985) 404.
7. R. A. BUBECK, D. J. BUCKLEY, D. J. KRAMER and H. J. BROWN, *J. Mater. Sci.* **26** (1991) 6249.
8. J. U. STARKE, H. GUST, G. H. MICHLER and P. EYERER, in preparation.
9. A. S. ARGON, R. E. COHEN, O. S. GEBIZLIOGLU and C. E. SCHWIER, in "Advances in Polymer Science 52/53", edited by H. H. Kausch (Springer Verlag, Heidelberg, 1983).
10. H. GUST and J. U. STARKE, in 14. Stuttgarter Kunststoff-Kolloquium (1995), pp. 6.3.
11. H. Y. SUE, *J. Mater. Sci.* **27** (1992) 3098.
12. A. LAZZERI and C. B. BUCKNALL, *ibid.* **28** (1993) 6799.
13. *Idem. Polymer* **36** (1995) 2895.
14. G. H. MICHLER, *Coll. Polym. Sci.* **264** (1986) 522.
15. *Idem. Kunststoffe* **81** (1991) 449.
16. *Idem. Acta Polym.* **44** (1993) 113.
17. G. H. MICHLER and J. U. STARKE, in "Toughened Plastics II: Science and Engineering", edited by C. K. Riew and A. J. Kinloch, to be published.
18. G. H. MICHLER, in "Electron Microscopy in Solid State Physics", Vol. 16, edited by H. Bethge and J. Heydenreich (Elsevier, Amsterdam, 1987), p. 386.
19. G. H. MICHLER, B. HAMANN and J. RUNGE, *Angew. Makromol. Chem.* **180** (1990) 169.
20. G. H. MICHLER, *Trends Polym. Sci.* **3** (1995) 124.
21. R. C. CIESLINSKI, *J. Mater. Sci. Lett.* **11** (1992) 813.
22. E. J. KRAMER and L. L. BERGER, in "Advances in Polymer Science 91/92", edited by H.H. Kausch (Springer Verlag, Berlin, Heidelberg, 1990).
23. J. U. STARKE, G. SCHULZE and G. H. MICHLER, in preparation.
24. G. H. MICHLER, *Makromol. Chem. Macromol. Symp.* **41** (1991) 39.
25. T. C. B. MC LEISH, C. J. G. PLUMMER and A. M. DONALD, *Polymer* **30** (1989) 1651.

Received 18 October
and accepted 20 November 1995